

# Supplementary materials

## Potassic-Hastingsite from the Kedrovyy District (East Siberia, Russia): Petrographic Description, Crystal Chemistry, Spectroscopy, and Thermal Behavior

Ekaterina Kaneva<sup>1,2,\*</sup>, Tatiana Radomskaya<sup>1,2</sup>, Roman Shendrik<sup>1</sup>, Victor Chubarov<sup>1</sup> and Victoria Danilovsky<sup>3</sup>

<sup>1</sup> Vinogradov Institute of Geochemistry, Siberian Branch of the Russian Academy of Sciences, Irkutsk, 664033, Russia; taniaojigova@mail.ru (T.R.); r.shendrik@gmail.com (R.S); chubarov@igc.irk.ru (V.C)

<sup>2</sup> Department of Subsoil Use, Irkutsk National Research Technical University, Irkutsk, 664074, Russia

<sup>3</sup> Sobolev Institute of Geology and Mineralogy, Siberian Branch of the Russian Academy of Sciences, Novosibirsk, 630090, Russia; victoria.saratovkina@gmail.com (V.D)

\* Correspondence: kev604@mail.ru

**Table S1.** Anisotropic atomic displacement parameters ( $\text{\AA}^2$ ) of potassic-hastingsite sample.

Site	Atom	U11	U22	U33	U23	U13	U12
A	K <sup>+</sup>	0.0603(5)	0.0299(5)	0.0821(6)	0	0.0591(5)	0
A2	K <sup>+</sup>	0.0603(5)	0.0299(5)	0.0821(6)	0	0.0591(5)	0
M1	Fe <sup>2+</sup>	0.01577(12)	0.01636(11)	0.01176(11)	0	0.00493(9)	0
M2	Fe <sup>2+</sup> , Fe <sup>3+</sup> , Mg <sup>2+</sup>	0.01278(12)	0.01145(12)	0.01104(12)	0	0.003644(8)	0
M3	Fe <sup>2+</sup>	0.01548(16)	0.01188(15)	0.01265(15)	0	0.00245(12)	0
M4	Ca <sup>2+</sup>	0.01854(16)	0.01422(15)	0.01723(16)	0	0.00921(12)	0
T1	Si <sup>4+</sup> , Al <sup>3+</sup>	0.01169(14)	0.01151(14)	0.00990(14)	- 0.00012(11)	0.00276(11)	- 0.00072(11)
T2	Si <sup>4+</sup>	0.01184(14)	0.01123(13)	0.00989(14)	0.00031(11)	0.00359(10)	- 0.00057(11)
O1	O <sup>2-</sup>	0.0144(4)	0.0164(4)	0.0121(4)	-0.0012(3)	0.0036(3)	-0.0019(3)
O2	O <sup>2-</sup>	0.0121(3)	0.0158(4)	0.0132(4)	0.0002(3)	0.0028(3)	0.0002(3)
O3	O <sup>2-</sup> , F <sup>-</sup>	0.0116(5)	0.0149(5)	0.0134(5)	0	0.0020(5)	0
	Cl <sup>-</sup>	0.0179(5)	0.0146(5)	0.0141(5)	0	0.0050(4)	0
O4	O <sup>2-</sup>	0.0195(4)	0.0143(4)	0.0155(4)	-0.0012(3)	0.0075(3)	-0.0030(3)
O5	O <sup>2-</sup>	0.0146(4)	0.0185(4)	0.0132(4)	0.0052(3)	0.0031(3)	0.0007(3)
O6	O <sup>2-</sup>	0.0154(4)	0.0181(4)	0.0154(4)	-0.0042(3)	0.0047(3)	0.0007(3)
O7	O <sup>2-</sup>	0.0180(5)	0.0185(5)	0.0225(6)	0	0.0059(5)	0

**Table S2.** Unit cell parameters of the studied potassic-hastingsite as a function of T.

T (°C)	<i>a</i> (Å)	<i>b</i> (Å)	<i>c</i> (Å)	$\beta$ (°)	<i>V</i> (Å <sup>3</sup> )
30	9.975(2)	18.282(5)	5.364(2)	104.97(3)	944.9(4)
50	9.977(2)	18.294(5)	5.359(2)	104.93(3)	945.0(4)
100	9.985(2)	18.304(5)	5.358(2)	104.98(3)	946.1(4)
150	9.986(2)	18.308(5)	5.364(2)	104.95(3)	947.4(4)
200	9.992(2)	18.312(5)	5.366(2)	104.92(3)	948.7(4)
250	9.997(2)	18.319(5)	5.365(2)	104.90(3)	949.4(4)
300	9.998(2)	18.325(5)	5.364(2)	104.83(3)	949.9(4)
350	10.001(2)	18.337(5)	5.364(2)	104.88(3)	950.9(4)
400	9.998(2)	18.336(5)	5.363(2)	104.81(3)	950.5(4)
450	9.995(2)	18.342(5)	5.361(2)	104.82(3)	950.2(4)
500	9.992(2)	18.359(5)	5.358(2)	105.07(3)	949.0(4)
550	9.979(2)	18.372(5)	5.352(2)	105.12(3)	947.2(4)
600	9.957(2)	18.354(5)	5.350(2)	104.96(3)	944.6(4)
650	9.952(2)	18.357(5)	5.353(2)	104.96(3)	944.8(4)
700	9.949(2)	18.351(5)	5.355(2)	104.93(3)	944.7(4)
750	9.948(2)	18.327(5)	5.363(2)	104.91(3)	944.9(4)
700	9.941(2)	18.307(5)	5.355 (2)	104.96(3)	941.5(4)
600	9.927(2)	18.269(5)	5.355(2)	104.88(3)	938.5(4)
500	9.914(2)	18.266(5)	5.355(2)	104.89(3)	937.1(4)
400	9.906(2)	18.254(4)	5.354(2)	104.97(3)	935.1(4)
300	9.898(2)	18.253(5)	5.345(2)	105.05(3)	932.6(4)
200	9.887(2)	18.252(5)	5.334(2)	105.05(3)	929.5(4)
100	9.876(2)	18.236(4)	5.336(2)	105.02(3)	928.3(4)
30	9.870(2)	18.207(4)	5.331(2)	105.03(3)	925.4(4)

**Table S3.** X-ray powder diffraction data *vs* temperature for studied potassic-hastingsite.

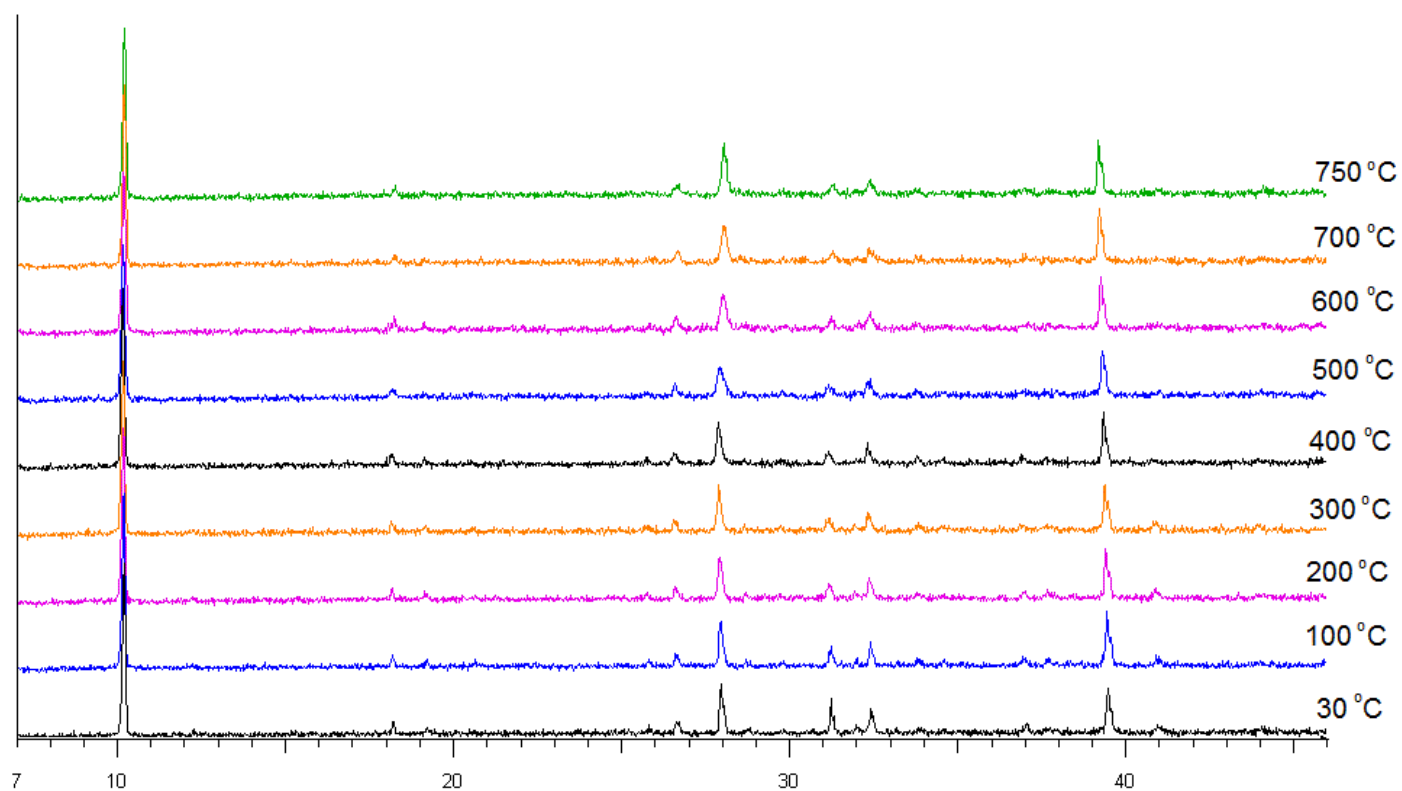
<i>hkl</i>	30 °C		50 °C		100 °C		150 °C		200 °C		250 °C		300 °C		350 °C		400 °C		450 °C		500 °C		550 °C	
	<i>I</i>	<i>d</i>	<i>I</i>	<i>d</i>	<i>I</i>	<i>d</i>	<i>I</i>	<i>d</i>	<i>I</i>	<i>d</i>	<i>I</i>	<i>d</i>	<i>I</i>	<i>d</i>	<i>I</i>	<i>d</i>	<i>I</i>	<i>d</i>	<i>I</i>	<i>d</i>	<i>I</i>	<i>d</i>	<i>I</i>	<i>d</i>
110	100	8.560	100	8.574	100	8.853	100	8.571	100	8.583	100	8.594	100	8.597	100	8.589	100	8.581	100	8.599	100	8.582	100	8.583
200	7	4.835	7	4.827	8	4.831	8	4.836	7	4.842	7	4.849	8	4.832	7	4.838	8	4.843	7	4.833	6	4.835	6	4.821
040	5	4.572	4	4.582	5	4.588	6	4.585	5	4.592	4	4.599	5	4.600	4	4.600	4	4.587	3	4.586	3	4.590	4	4.598
150	6	3.430	6	3.426	5	3.427	5	3.428	4	3.435	5	3.435	5	3.432	5	3.431	5	3.435	3	3.433	3	3.438	5	3.426
240	10	3.319	11	3.319	10	3.324	9	3.326	10	3.324	11	3.327	10	3.328	12	3.331	9	3.331	11	3.329	11	3.328	10	3.322
310	35	3.166	36	3.166	35	3.169	36	3.170	35	3.173	33	3.175	36	3.175	33	3.177	33	3.176	32	3.175	27	3.171	28	3.165
$\bar{3}11$	5	3.083	4	3.087	4	3.085	4	3.092	4	3.085	3	3.091	3	3.089	3	3.089	3	3.090	4	3.091	3	3.085		
221	3	2.980	4	2.977	3	2.979	5	2.986	3	2.980	4	2.979	4	2.988	5	2.982	3	2.983	4	2.982	3	2.980	3	2.979
330	19	2.844	20	2.844	15	2.846	12	2.847	13	2.849	12	2.849	12	2.850	12	2.851	11	2.851	11	2.852	10	2.849	10	2.847
151	19	2.743	19	2.742	18	2.743	19	2.743	16	2.746	16	2.746	14	2.750	16	2.749	14	2.748	15	2.750	16	2.749	15	2.747
061	5	2.630	6	2.634	6	2.633	5	2.634	5	2.633	5	2.635	5	2.633	6	2.636	7	2.637	7	2.635	7	2.636	7	2.636
400	10	2.413	8	2.414	8	2.417	7	2.414	7	2.417	6	2.418	5	2.419	5	2.420	6	2.419	7	2.420	5	2.418	7	2.417
$35\bar{1}$	5	2.372	4	2.370	6	2.372	6	2.371	5	2.373	5	2.372	4	2.373	4	2.372	3	2.373	4	2.372				
171	7	2.190	8	2.190	8	2.191	9	2.193	8	2.193	9	2.194	9	2.194	6	2.196	4	2.198	4	2.189				
202	5	2.045	3	2.044	4	2.089	3	2.080	3	2.056	4	2.045	7	2.048	5	2.049	4	2.049	7	2.049				
461	7	1.670	6	1.671	6	1.672	3	1.672	5	1.673	6	1.673	7	1.676	3	1.702	5	1.676	6	1.664	6	1.667	8	1.667
480	6	1.658	3	1.658	5	1.658																		
600	5	1.605	4	1.605	6	1.606	5	1.608	6	1.609	7	1.609	3	1.610	3	1.610	5	1.611	3	1.605	4	1.604	3	1.603
402	4	1.572	5	1.572	5	1.573	4	1.574																
$26\bar{3}$	7	1.524	3	1.524	5	1.525	6	1.522	4	1.524	7	1.524	6	1.526	4	1.526	3	1.520	3	1.522	5	1.525		
$66\bar{1}$	8	1.457	8	1.459	8	1.459	7	1.458	7	4.460	5	1.460	5	1.462	6	1.463	3	1.463	5	1.459	3	1.459	3	1.459

Table S3. (contd.)

<i>hkl</i>	600 °C		650 °C		700 °C		750 °C		700 °C		600 °C		500 °C		400 °C		300 °C		200 °C		100 °C		30 °C	
	<i>I</i>	<i>d</i>	<i>I</i>	<i>d</i>	<i>I</i>	<i>d</i>	<i>I</i>	<i>d</i>	<i>I</i>	<i>d</i>	<i>I</i>	<i>d</i>	<i>I</i>	<i>d</i>	<i>I</i>	<i>d</i>	<i>I</i>	<i>d</i>	<i>I</i>	<i>d</i>	<i>I</i>	<i>d</i>	<i>I</i>	<i>d</i>
110	100	8.561	100	8.568	100	8.563	100	8.559	100	8.534	100	8.537	100	8.532	100	8.511	100	8.516	100	8.499	100	8.501	100	8.489
200	6	4.822	7	4.816	7	4.814	8	4.818	7	4.809	7	4.811	8	4.802	8	4.793	8	4.794	8	4.788	7	4.777	7	4.777
040	4	4.599	3	4.596	3	4.594	4	4.590	3	4.590	3	4.592	4	4.590	5	4.576	4	4.575	4	4.573	5	4.574	5	4.562
150	5	3.418	3	3.418	4	3.419	3	3.417	6	3.417	6	3.414	6	3.411	6	3.413	7	3.411	5	3.406	5	3.409	6	3.404
240	10	3.322	11	3.324	10	3.322	9	3.320	10	3.318	10	3.313	11	3.310	10	3.308	11	3.303	10	3.298	9	3.298	10	3.295
310	28	3.160	31	3.159	30	3.160	39	3.160	36	3.156	37	3.151	39	3.147	36	3.144	38	3.142	33	3.137	33	3.134	34	3.133
$\bar{3}11$																								
221	3	2.977													3	2.958	3	2.958						
330	10	2.845	10	2.842	8	2.841	9	2.842	10	2.839	11	2.835	12	2.835	11	2.828	12	2.828	13	2.823	13	2.822	14	2.817
151	15	2.746	13	2.746	9	2.744	12	2.745	14	2.742	14	2.741	15	2.739	14	2.736	13	2.734	14	2.732	15	2.730	16	2.727
061	7	2.636	8	2.635	4	2.633	4	2.637	7	2.633	5	2.627	7	2.629	6	2.626	6	2.623	6	2.621	5	2.620	6	2.618
400	7	2.413	5	2.413	6	2.413	5	2.413	5	2.413	6	2.411	6	2.403	6	2.402	5	2.399	7	2.399	6	2.393	7	2.396
35 $\bar{1}$			5	2.362	3	2.363	3	2.365					4	2.367	3	2.361					5	2.357	4	2.352
171			3	2.193	3	2.193	6	2.191	3	2.190	6	2.188	5	2.186	6	2.182	6	2.181	6	2.179	7	2.176	7	2.178
202	3	2.040	4	2.043	4	2.047	6	2.043	6	2.041	5	2.035	5	2.032	3	2.030	4	2.030					5	2.026
461	8	1.666	5	1.660							5	1.661	6	1.659	3	1.663	3	1.680	3	1.676				
480															3	1.652	4	1.652	6	1.656	6	1.651	6	1.652
600	3	1.601	5	1.601	5	1.609	6	1.606	6	1.607	6	1.604	6	1.600	3	1.593	5	1.592	4	1.593				
402																								
26 $\bar{3}$											3	1.532	5	1.530	3	1.518	4	1.527						
66 $\bar{1}$	4	1.458	5	1.459	4	1.459	3	1.458	6	1.458	4	1.457	5	1.453	7	1.452	5	1.451	7	1.449	5	1.445	3	1.444

**Table S4.** Coefficients of thermal expansion tensor ( $\alpha_{ij}$ ) of the studied potassic-hastingsite as a function of T and orientation of its eigenvectors with respect to unit cell axes. For the monoclinic system  $\alpha_{12} = \alpha_{23} = 0$ ,  $\alpha_{31} = \alpha_{13}$ , while  $\text{EV1} \angle b = \text{EV2} \angle a = \text{EV3} \angle b = 90^\circ$  and  $\text{EV2} \angle b = 0^\circ$ ;  $\text{EV1} \angle e_2 = \text{EV2} \angle e_1 = \text{EV3} \angle e_2 = 90^\circ$  and  $\text{EV2} \angle e_2 = 0^\circ$ .

T (°C)	$\alpha_{11}$	$\alpha_{22}$	$\alpha_{33}$	$\alpha_{13}$	EV1<a	EV1<c	EV3<a	EV3<c	EV1<e <sub>1</sub>	EV1<e <sub>3</sub>	EV3<e <sub>1</sub>	EV3<e <sub>3</sub>
30	$3.39 \times 10^{-6}$	$2.21 \times 10^{-5}$	$-1.55 \times 10^{-5}$	$-2.90 \times 10^{-5}$	68.95	158.95	35.98	54.02	54.02	144.02	35.98	54.02
50	$5.95 \times 10^{-6}$	$1.74 \times 10^{-5}$	$-8.60 \times 10^{-6}$	$-1.71 \times 10^{-5}$	71.50	161.50	33.48	56.53	56.53	146.53	33.48	56.53
100	$1.10 \times 10^{-5}$	$9.26 \times 10^{-6}$	$2.83 \times 10^{-6}$	$2.07 \times 10^{-6}$	61.47	28.53	166.47	76.47	76.47	13.53	166.47	76.47
150	$1.35 \times 10^{-5}$	$5.44 \times 10^{-6}$	$7.53 \times 10^{-6}$	$9.64 \times 10^{-6}$	38.63	51.37	143.59	53.59	53.59	36.42	143.59	53.59
200	$1.33 \times 10^{-5}$	$4.56 \times 10^{-6}$	$7.38 \times 10^{-6}$	$9.62 \times 10^{-6}$	38.69	51.31	143.59	53.59	53.59	36.41	143.59	53.59
250	$1.06 \times 10^{-5}$	$5.45 \times 10^{-6}$	$4.12 \times 10^{-6}$	$5.41 \times 10^{-6}$	45.60	44.40	150.45	60.45	60.45	29.55	150.45	60.45
300	$5.57 \times 10^{-6}$	$7.11 \times 10^{-6}$	$-7.39 \times 10^{-7}$	$-2.81 \times 10^{-7}$	102.29	167.71	2.55	87.45	87.45	177.45	2.55	87.45
350	$-1.21 \times 10^{-6}$	$8.71 \times 10^{-6}$	$-5.88 \times 10^{-6}$	$-5.38 \times 10^{-6}$	71.59	161.59	33.26	56.74	56.74	146.74	33.26	56.74
400	$-8.97 \times 10^{-6}$	$9.59 \times 10^{-6}$	$-1.02 \times 10^{-5}$	$-8.46 \times 10^{-6}$	61.94	151.94	42.94	47.06	47.06	137.06	42.94	47.06
450	$-1.67 \times 10^{-5}$	$9.25 \times 10^{-6}$	$-1.27 \times 10^{-5}$	$-8.77 \times 10^{-6}$	53.59	143.59	51.34	38.66	38.66	128.66	51.34	38.66
500	$-2.30 \times 10^{-5}$	$7.36 \times 10^{-6}$	$-1.27 \times 10^{-5}$	$-6.19 \times 10^{-6}$	40.14	130.14	64.84	25.16	25.16	115.16	64.84	25.16
550	$-2.64 \times 10^{-5}$	$3.77 \times 10^{-6}$	$-9.69 \times 10^{-6}$	$-1.25 \times 10^{-6}$	19.25	109.25	85.76	4.23	4.23	94.24	85.76	4.23
600	$-2.51 \times 10^{-5}$	$-1.52 \times 10^{-6}$	$-3.24 \times 10^{-6}$	$4.85 \times 10^{-6}$	3.07	93.07	101.95	11.95	11.95	78.05	101.95	11.95
650	$-1.71 \times 10^{-5}$	$-8.34 \times 10^{-6}$	$6.77 \times 10^{-6}$	$1.02 \times 10^{-5}$	5.34	84.67	110.32	20.33	20.33	69.68	110.32	20.33
700	$7.52 \times 10^{-8}$	$-1.64 \times 10^{-5}$	$2.03 \times 10^{-5}$	$1.24 \times 10^{-5}$	10.47	79.53	115.42	25.42	25.42	64.58	115.42	25.42
750	$2.89 \times 10^{-5}$	$2.51 \times 10^{-5}$	$3.70 \times 10^{-5}$	$8.20 \times 10^{-6}$	16.91	73.10	121.80	31.80	31.80	58.20	121.80	31.80



**Figure S1.** Selected XRPD patterns of potassic-hastingsite showing the evolution of the diffraction patterns collected during the heating experiment. In all patterns the 7–45°  $2\theta$  range is reported.

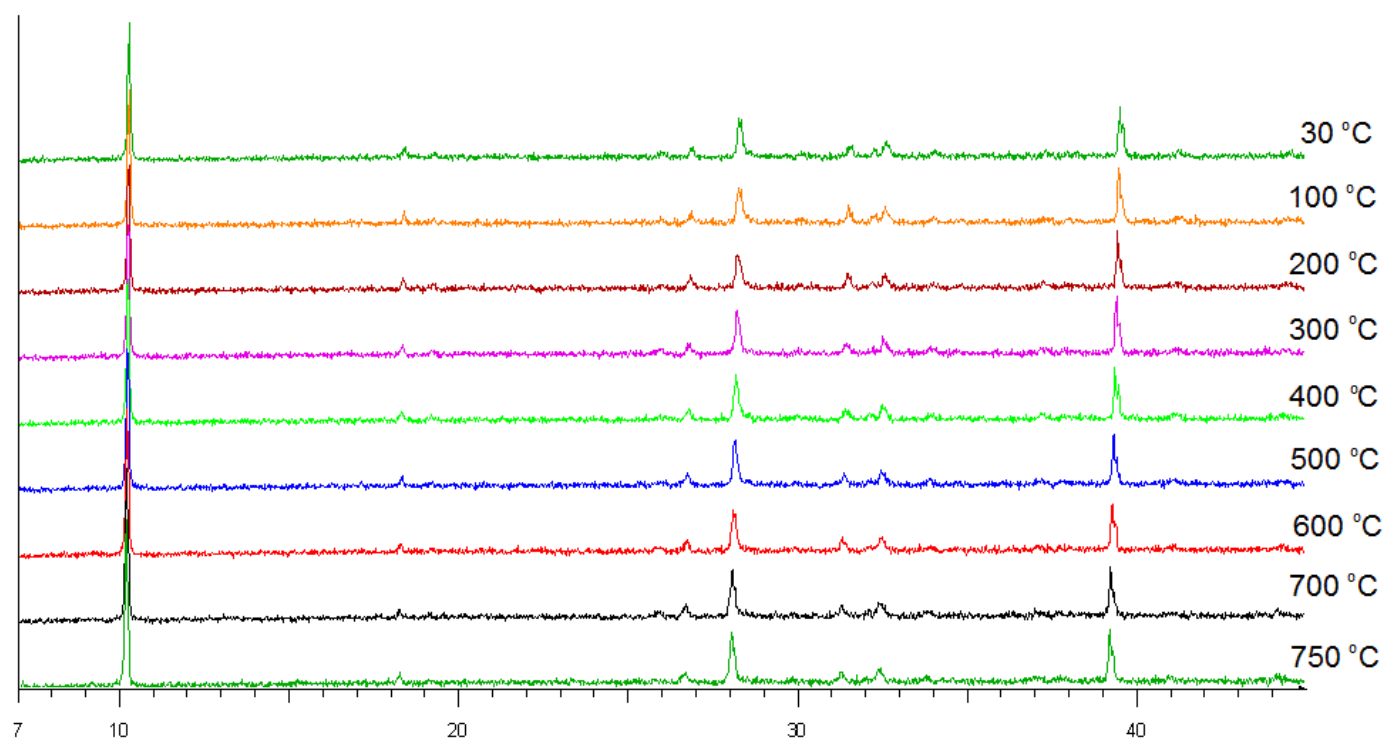


**Figure S2.** XRPD patterns of potassic-hastingsite showing the evolution of the diffraction patterns collected during the cooling experiment. In all patterns the 7–45°  $2\theta$  range is reported.

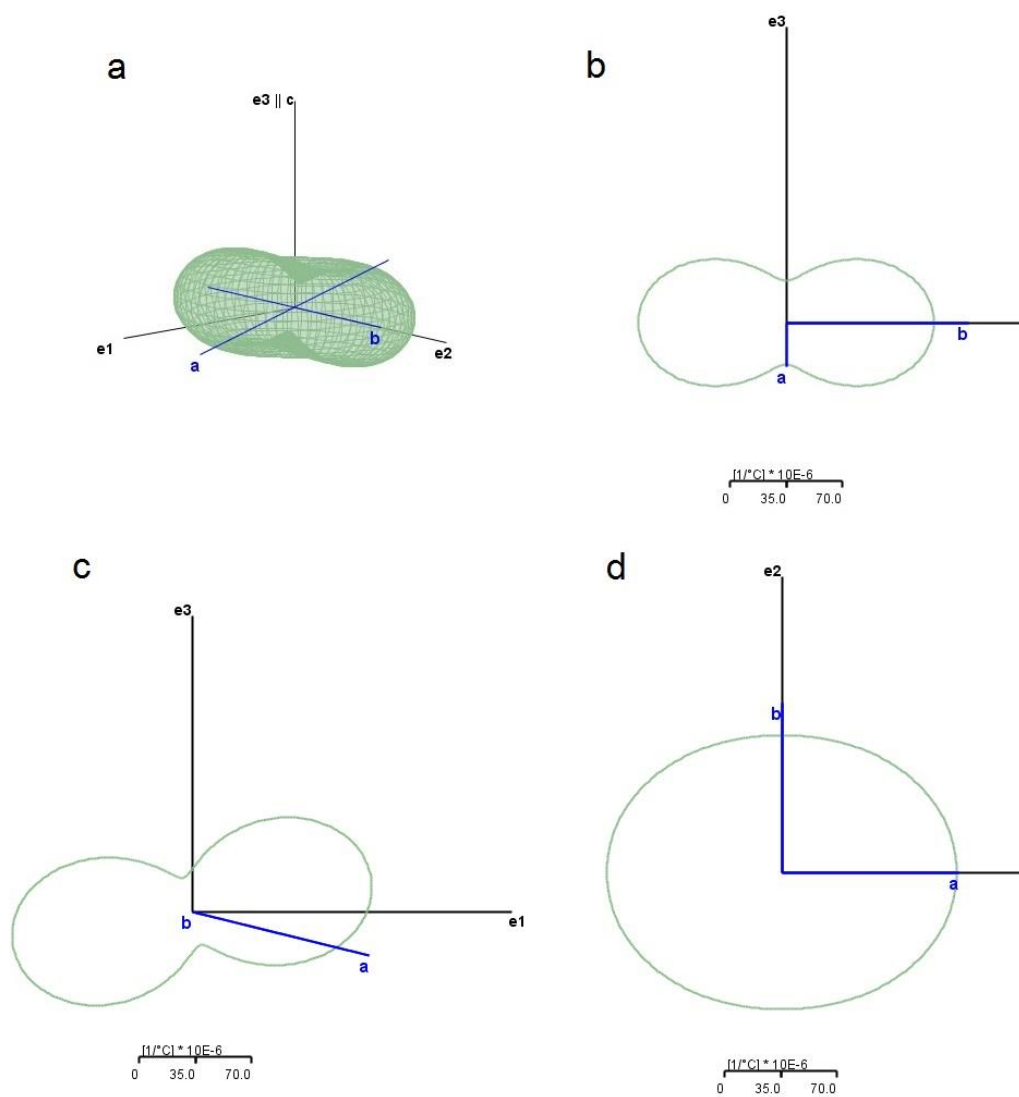


**Figure S3.** Graphical representation of the thermal expansion tensor of the potassic-hastingsite at 100°C: **a)** 3D view; **b)**  $e_2 - e_3$  section; **c)**  $e_1 - e_3$  section; **d)**  $e_1 - e_2$  section. The green and red colours represent directions of positive and negative expansion, respectively.

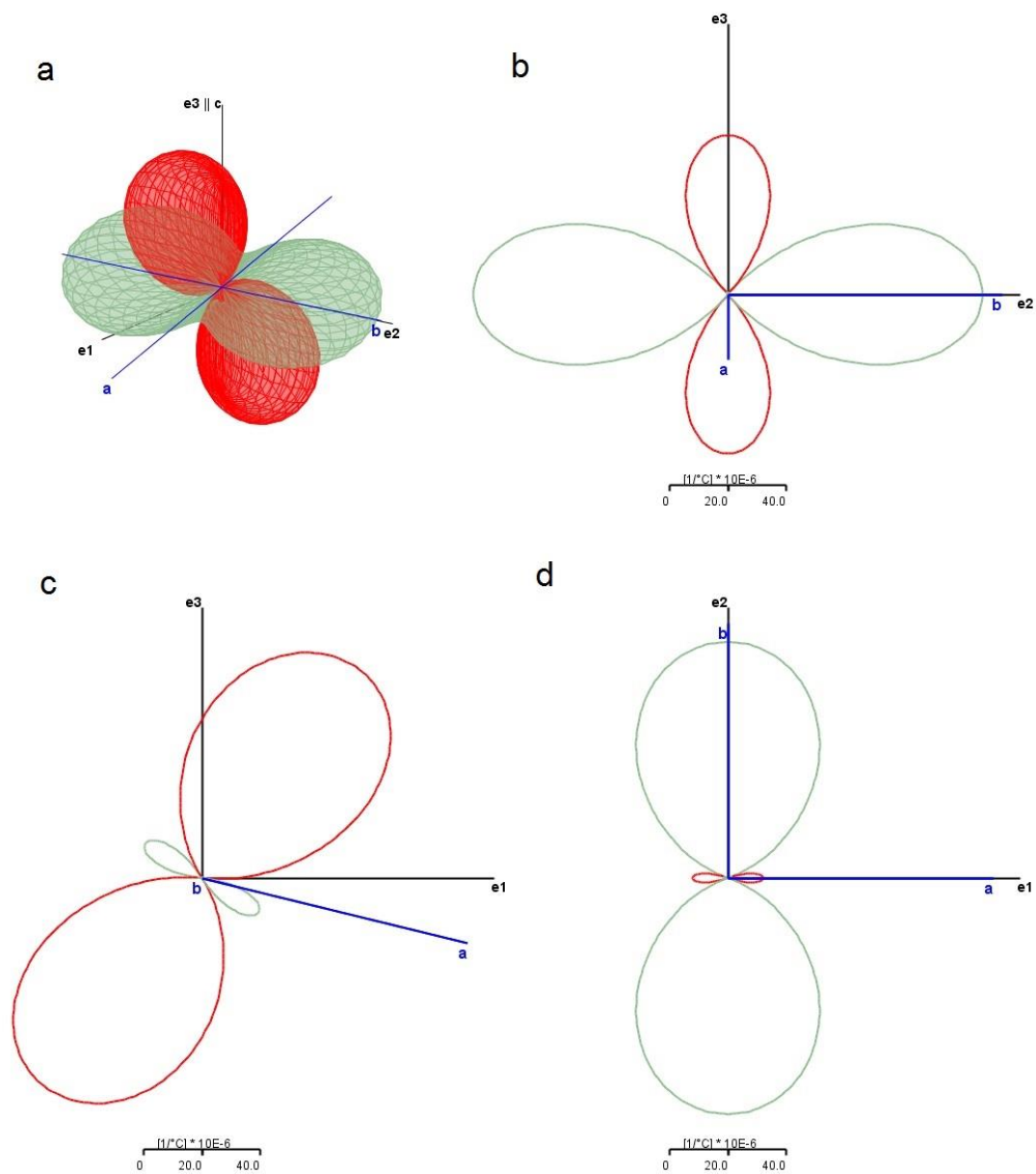


**Figure S4.** Graphical representation of the thermal expansion tensor of the potassic-hastingsite at 350°C: **a)** 3D view; **b)**  $e_2 - e_3$  section; **c)**  $e_1 - e_3$  section; **d)**  $e_1 - e_2$  section. The green and red colours represent directions of positive and negative expansion, respectively.



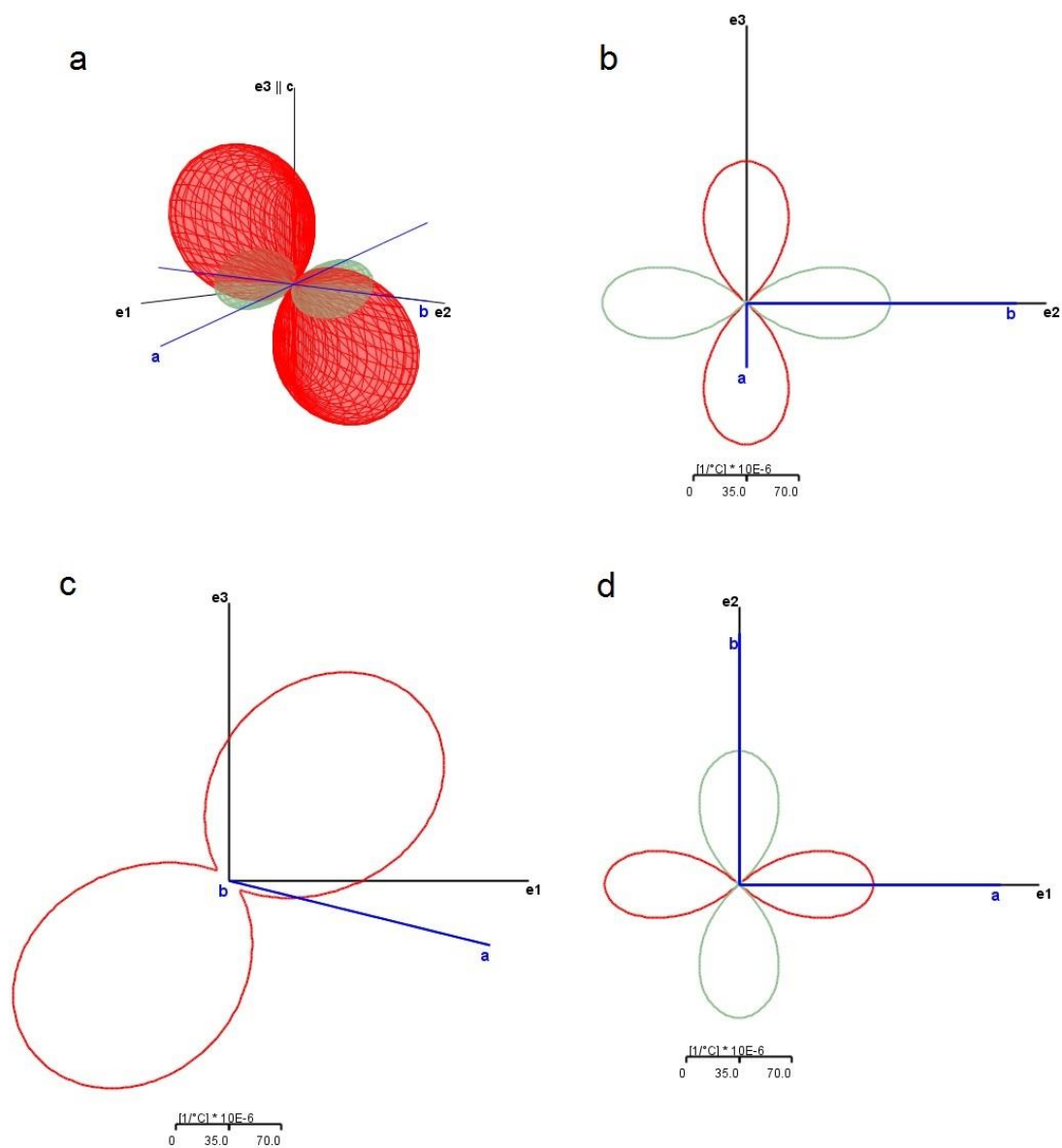


**Figure S5.** Graphical representation of the thermal expansion tensor of the potassic-hastingsite at 400°C: **a)** 3D view; **b)**  $e_2 - e_3$  section; **c)**  $e_1 - e_3$  section; **d)**  $e_1 - e_2$  section. The green and red colours represent directions of positive and negative expansion, respectively.

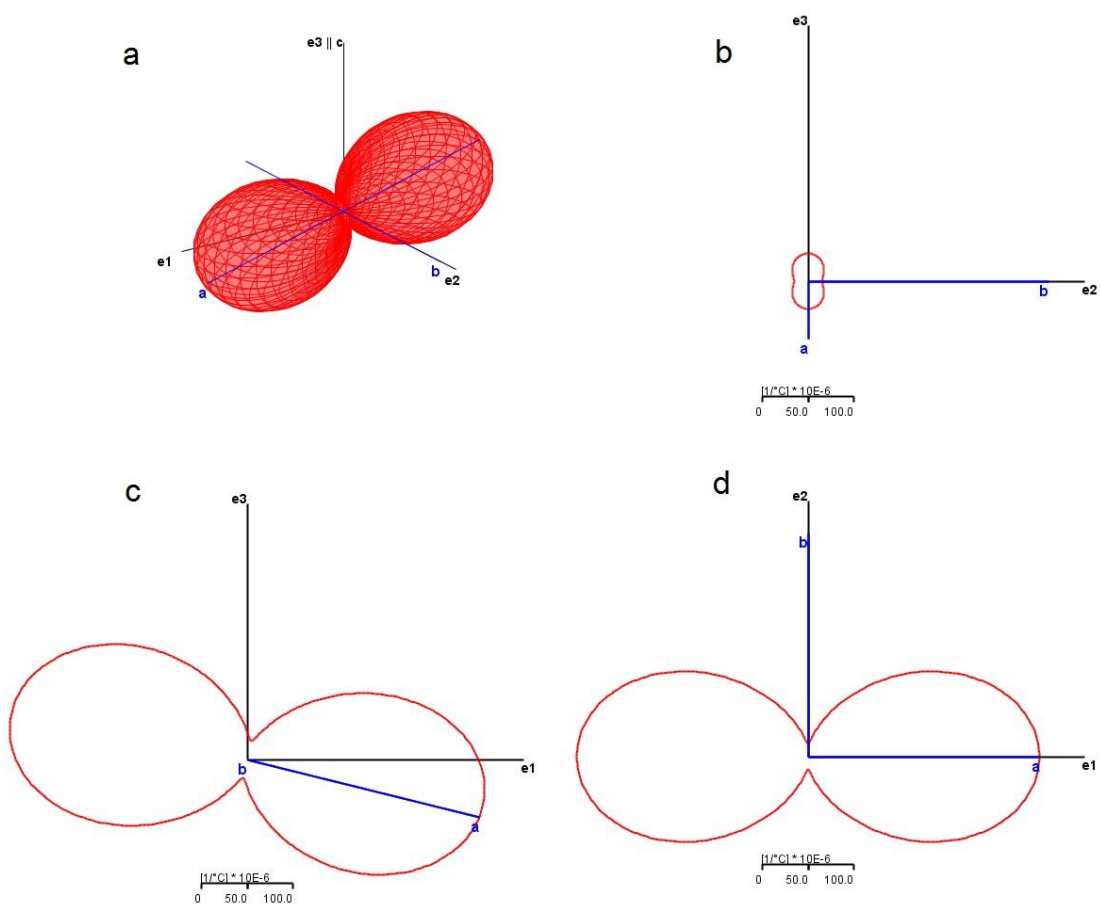


**Figure S6.** Graphical representation of the thermal expansion tensor of the potassic-hastingsite at 600°C: **a)** 3D view; **b)**  $e_2 - e_3$  section; **c)**  $e_1 - e_3$  section; **d)**  $e_1 - e_2$  section. The green and red colours represent directions of positive and negative expansion, respectively.

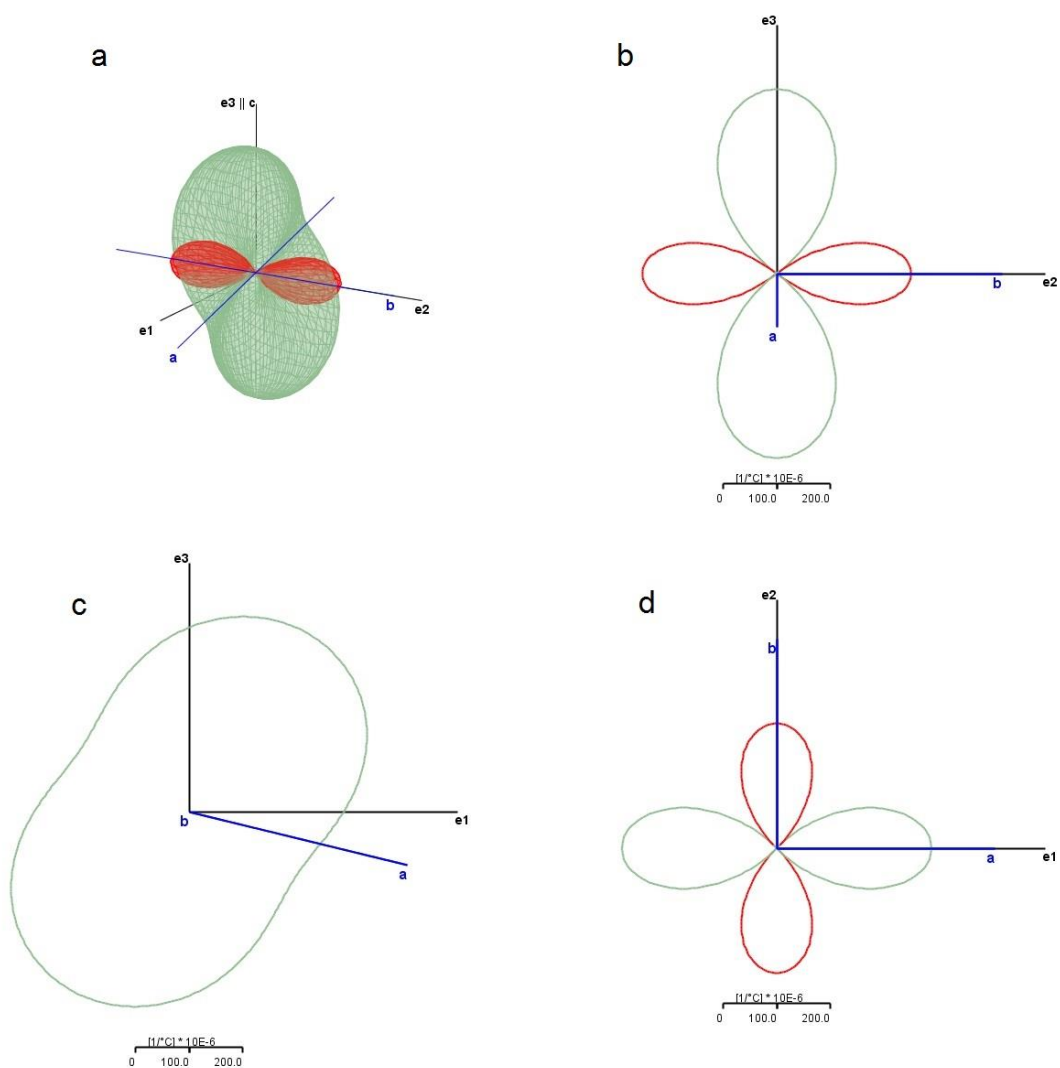


**Figure S7.** Graphical representation of the thermal expansion tensor of the potassic-hastingsite at 750°C: **a)** 3D view; **b)**  $e_2 - e_3$  section; **c)**  $e_1 - e_3$  section; **d)**  $e_1 - e_2$  section. The green and red colours represent directions of positive and negative expansion, respectively.